Journal of Asian Concrete Federation

journal homepage: https://jacf.sfulib3.publicknowledgeproject.org/index.php/jacf

Chloride diffusion investigation under different magnitudes of hydrostatic pressure for pre-cracked concrete

Jie Ren[a*], Lei Guo[a], Chuangzhou Wu[b*]

[a] College of Pipeline and Civil Engineering, China University of Petroleum (East China), Qingdao, 266580, China
[b] Institute of Port, Coastal, and Offshore Engineering, Ocean College, Zhejiang University, Zhoushan 316021, China

ABSTRACT

The service life of the reinforced concrete structure in the marine environment can be impaired significantly due to chloride-induced corrosion. However, how the chloride diffusion in pre-cracked concrete structures is affected by the hydrostatic pressure is poorly understood. This study experimentally examined the effect of hydrostatic pressure on the chloride diffusion in pre-cracked concrete. Cracks with five different widths, i.e., 20 μm, 40 μm, 60 μm, 80 μm, and 100 μm, were manually created each using a splitting tensile apparatus. The chloride diffusion in the concrete with a certain crack was then studied under four different hydrostatic pressures of 0 MPa, 0.1 MPa, 0.3 MPa, and 0.5 MPa. Experimental results show that the chloride diffusion in concrete with a crack greatly relies on both the hydrostatic pressure and the crack width. The chloride concentration increases as the hydrostatic pressure grows, particularly for the wider cracks with width ranging from 60 μm to 100 μm. Unexpectedly, the hydrostatic pressure has a negligible effect on the chloride distribution in the concrete with a crack width no larger than 40 μm. Thus, the critical crack width is between 40 and 60 μm. Both the chloride diffusion coefficient and the chloride concentration of concrete at a certain depth increased gradually as the hydrostatic pressure increased, the latter of which exhibited a linear relationship with the hydrostatic pressure The experimental findings enrich our understanding of the behavior of pre-cracked concrete when exposed to chloride-induced corrosion at different depths of marine environments.

Keywords: Concrete cracking; Hydrostatic pressure; Diffusion coefficient; Chloride transportation

1. Introduction

The performance of reinforced concrete structures built and served in marine environments are often degraded due to chloride-induced corrosion. Chloride ion penetration into concrete depends on a number of variables, such as chloride ion concentration, corresponding microstructures and properties of concrete and the magnitude of hydrostatic pressure [1-7]. On the one hand, concrete structures are unavoidably cracked due to internal deformation and external loadings during their service life. The presence of cracks in the concrete accelerates the corrosion process of the steel reinforcement. On the other hand, water pressure affects substantially the chloride penetration process into concrete with cracks whose hydraulic properties are heavily stress dependent. Therefore, understanding the behaviour of chloride diffusion in concrete with cracks under various hydrostatic pressure is critical to assess and predict the long-term durability of marine concrete structures, particularly for those built in the deep-sea environments [6, 8, 9].

The effect of cracks on the chloride penetration of concrete has attracted numerous investigations recently [6, 10-18]. Aldea et al. [16] reported that the chloride permeability increased with increased crack widths and the water permeability was much more sensitive than that of chlorides. Olga and Hooton [18], however, reported that chloride diffusion was independent of both crack width and crack wall roughness. François et al. [17] reported that the chloride diffusion perpendicular to the crack walls with wide cracks (width $\geqslant$ 205 μm) was similar to that of the surface. For the cracks running through the

* Corresponding author: Chuangzhou Wu(arc_wu@zju.edu.cn), Jie Ren(jie.ren@upc.edu.cn)

DOI http://dx.doi.org/10.18702/acf.2026.12.3.27

Received: 22-May-2026; Revised: 15-Jun-2026; Accepted: 24-Jun-2026; Published online: 31-Jul-2026

ISSN 2465-7964, eISSN 2465-7972. Copyright © Asian Concrete Federation, All rights reserved.

specimens, the diffusion coefficient in the crack under steady-state conditions was assumed to equal the diffusion coefficient in free solution [19, 20]. Therefore, it is apparent that cracks in concrete greatly affect the durability of reinforced concrete structures with some inconsistent findings from previous literature. Moreover, Liu et al. [21-24] studied the migration mechanism of chloride in cracked concrete by numerical simulation, which provided a new idea for the durability design of concrete. In theory, stability of deep-sea concrete-made engineering infrastructures is closely associated with the concrete durability under a high hydrostatic pressure environment. However, the coupled effect of hydrostatic pressure and crack widths on the penetration of chloride in cracked concrete has been rarely explored.

This paper reports experimental studies on chloride diffusion in the pre-cracked concrete with different degrees of hydrostatic pressure. The crack of a desired width in the concrete specimen was manually created using a controlled splitting tensile apparatus and maintained during the chloride penetration process in cracked concrete. The average crack widths varied from 20 μm to about 100 μm. The selected crack widths were based on other studies [6, 25] and practical circumstances. Moreover, the effect of hydrostatic pressure on the diffusion coefficient values of the cracked concrete was also examined.

2. Overview of Experiments and Specimen

2.1. Sample preparation

Fig. 1 illustrates the experimental configuration for exploring the chloride transport into the cracked concrete samples under various magnitudes of hydrostatic pressure. An air pressure machine was employed to apply four different hydrostatic pressures of 0 MPa, 0.1 MPa, 0.3 MPa and 0.5 MPa on the cracked concrete, and the highest hydrostatic pressure simulated the marine environment in depth up to 50m [26, 27]. The concrete specimen exhibited a ring profile with an inner radius of 50 mm, outer radius of 200 mm, and height of 80 mm (Fig. 1b). The concrete mixture consisted of cement, water, sand, aggregates, and water reducing agent in the ratio of 1:0.38:1.56:2.66:0.012 by mass, which complied with the Chinese Standard, JGJ55-2011 [28]. The cement type was P.II 52.5, with an apparent density of 3150 kg/m^3. The size of coarse aggregate ranged from 5 mm to 20 mm with continuous grading, and its apparent density was 2630 kg/m^3. The apparent density of sand was 2.64 g/cm^3 with a water proportion of 3.7%. The type of the water reducing agent was HP4000A with a water reduction ratio of 27.5%. The concrete specimens were prepared by mixing the raw materials for 3 mins followed by adding water (the water reducing agent was dissolved in water first) into the dry mixture and the whole mixture was mixed for another 3 mins before casting into the cylindrical molds. Then the specimens were vibrated on a vibrating table for 30 seconds and cured under standard condition (20±2 ° C, RH ⩾ 95%) for 28 days before further testing.

The uniaxial compressive strength of the concrete was 50.5 ± 0.5 MPa and 59.1 ± 0.3 MPa after 14 and 28 days of curing, respectively. The tensile strength of the concrete was respectively 5.36 ± 0.44 MPa and 6.87 ± 0.27 MPa after 14 and 28 days. Twenty concrete samples were prepared from a single batch for the concrete mixtures after 14 and 28 days of curing, respectively. The concrete mixtures were cast in steel molds and compacted using a mechanical vibrator.

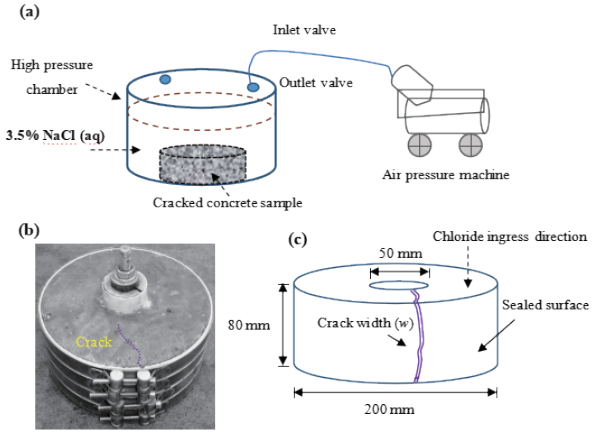


Fig. 1. Experimental configuration: (a) illustration of chloride penetration test on the cracked concrete under different levels of hydrostatic pressure, also known as pressurized salt bath testing, (b) concrete samples with a crack of a specified width (w), and (c) dimensions of the crack concrete sample with surface sealed.

2.2. Sample pre-cracking

Cracks with five different widths of 20 μm, 40 μm, 60 μm, 80 μm, and 100 μm in the ring concrete sample was created by a controlled splitting tensile apparatus. To be specific, the cylindrical specimens were first loaded in a deformation-controlled indirect tension device to generate cracking with predetermined crack widths. The splitting tensile apparatus was controlled at a constant displacement rate of 0.02 mm/min via a vertical loading mode. In order to monitor the crack widths, a crack width gauge, i.e., DJCK-2 Type, was used. Based on our preliminary studies, the corresponding crack width ranges (20-100 μm) could be obtained when the loading stress increases gradually up to 60% to 80% of the ultimate tensile strength (6.87 ± 0.27 MPa). A certain obtained crack usually had a uniform width throughout the whole specimen. Based on the resolution of the gauge, the standard deviations of the crack widths should be no more than 0.01 mm. After cutting, the lateral surfaces of ring concrete sample were tightly sealed with two layers of epoxy resin coats to ensure that the chlorides flow through the ring concrete crack in radial direction (Fig. 1c). Detailed procedures regarding the coating and how to maintain the crack widths can be referred to another study [29].

3 Results and analysis

3.1. Chloride concentration quantification

The chloride concentration in concrete is estimated

through the Volhard method. The powdered concrete samples normal to the crack surface are used to extract acid-soluble chloride contents, as shown in Fig. 1c. The chloride diffusion is calculated by fitting the experimentally-measured curves. The penetration of chloride into concrete is assumed one-dimensional in a semi-infinite medium complying with Fick's second law of pure diffusion [30, 31]:

$$\frac{\partial C}{\partial t} = D_a \frac{\partial^2 C}{\partial x^2} \quad (1)$$

Solve Eq. (1):

$$C(x,t) = C_0 + (C_s - C_0)\left[1 - erf\left(\frac{x}{2\sqrt{D_a t}}\right)\right] \quad (2)$$

where C(x,t) is the chloride concentration at distance x from the exposed surface, C_s is the surface chloride concentration, D_a is the apparent chloride diffusion coefficient, is the exposure time, and erf is the error function [30, 32]. The values of D_a and C_s are determined from fitting the measured chloride profile. The corresponding results are presented in Section 3.4.

3.2 Effect of crack width on chloride diffusion

Fig. 2 shows the chloride concentration of the ring concrete sample with different crack widths under four magnitudes of hydrostatic pressure. As the hydrostatic pressure grows from 0 to 0.5 MPa, remarkable difference in chloride concentration (C) occurs between the crack width increasing from 20 μm to 40 μm and that from 60 μm to 100 μm. The chloride concentration (C) (0.025% to 0.041%) for the crack width of 20 μm to 40 μm is substantially lower than that of 60 μm to100 μm (0.19% to 0.36%), particularly for those close to the crack surface. The discrepancy decreases gradually as the penetration depth (d) from the crack surface increases. This indicates that the crack width remarkably affects the chloride transport in concrete and the influence degree decreases with the increasing penetration depth. The effect of the crack width is much less pronounced when the width is around 20 μm to 40 μm. Similarly, minor difference is found given the crack width ranging between 60 μm and 100 μm. Therefore, a critical crack width exists beyond which the chloride transportation in concrete is significantly influenced. The results are consistent with the findings reported from other studies [15, 33, 34]. In the study carried out by Wang et al. [12], it was also found that the chloride diffusion depth increased significantly when the crack width was 0.05 mm or greater, compared to that when the crack width was 0.03 mm or less. In that case, the threshold (the critical crack width) was about 0.03 -0.05 mm, close to the result from this research (40-60 μm). When the crack width is greater, there are more capillary pores available on the surface of cracks, making the ingress of water easier, and thus the chloride concentration was also higher. Under this condition, the chlorides in water are transported in diffusion mode with a diffusion coefficient in water of about 10^{-9} m^2/s (an increased crack width corresponds to a higher diffusion coefficient). Therefore, the concentration of chlorides at a certain depth was much greater when the crack width w was 60 μm or greater. The inflection points at a penetration depth of around 12.5 mm for the chloride concentration curves seen in the specimens with a crack width of 60, 80, and 100 μm also implies that there are multiple forces which control the chloride ingress.

It is also noteworthy that there are many microcracks invisible near the 60–100 μm cracks, which would increase the contact surface of binding matrix with water. During this process, some cementitious components such as C-S-H gels and Portlandite get dissolved via leaching. As a result, additional pores including capillary pores could have formed and a coarsened pore structure is then obtained within the original binding matrix in this area. For this study, the leaching process and formation of microcracks significantly enhanced the interstitial flow of pore fluids and ingress of external solution, leading to a higher chloride concentration.

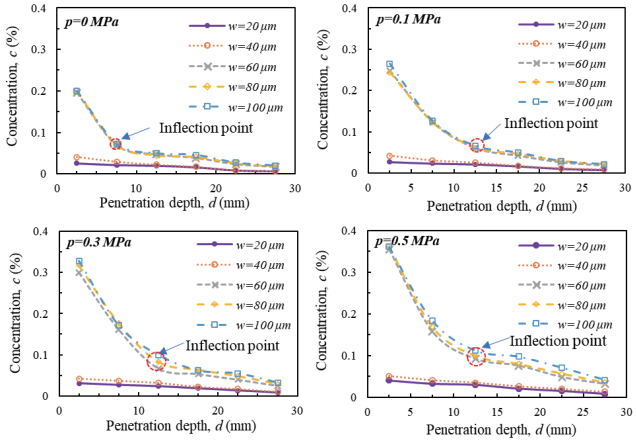


Fig. 2. Chloride concentration of the cracked concrete with different crack width (w) under various magnitudes of hydrostatic pressure (p)

3.3 Effect of hydrostatic pressure on chloride diffusion

Fig. 3 shows the effect of hydrostatic pressure on the chloride transport in concrete with different crack width. Appreciable difference can be found between the chloride concentration for the crack width from 20 μm to 40 μm and that for the crack width from 60 μm to 100 μm. The hydrostatic pressure only slightly affects the chloride transport in the concrete with the crack width from 20 μm to 40 μm, whereas the chloride concentration in concrete with crack width from 60 μm to 100 μm is strongly affected. Besides, it is obvious that the chloride concentration increases as the hydrostatic pressure increases, particularly for the region near the crack. This phenomenon can be explained by considering the fact that when there is an external hydraulic pressure applied to the crack, the water infiltration depth increases and thus the corresponding rate of chloride penetration becomes higher, leading to higher concentration of chlorides at a certain depth [6]. The slope of the curves for the crack width from 20 μm to 40 μm is around 0.01 to 0.03 whereas it increases to around 0.03 to 0.3 for the crack width from 60 μm to 100 μm. The slope approaches the maximum value of 0.3 at the depth of 2.5 cm.

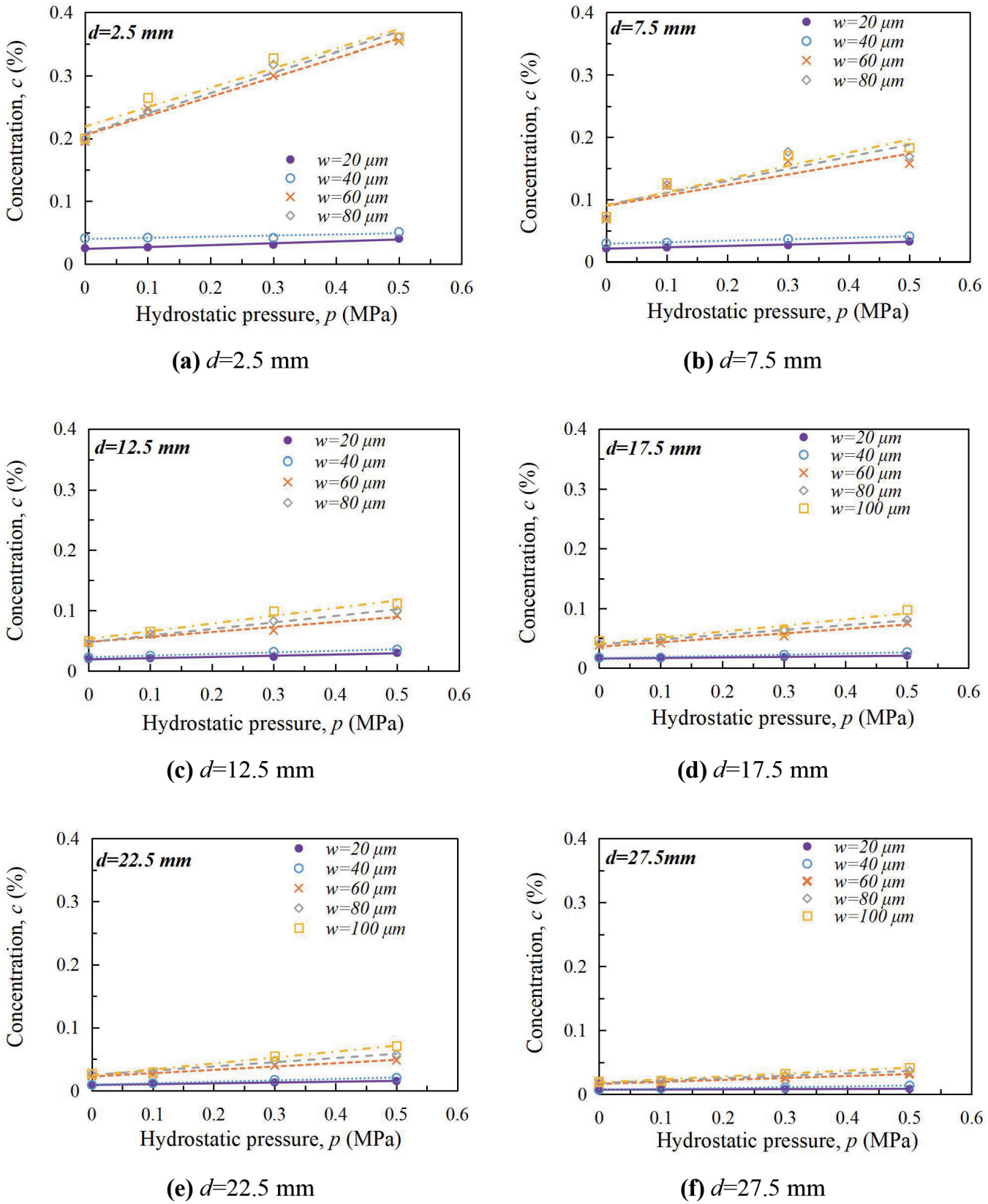


Fig. 3. Effect hydrostatic pressure (p) on chloride distribution in concrete with different crack width (w). d is the penetration depth.

The hydrostatic pressure has a great effect on the chloride transport in concrete with the crack width from 60 μm to 100 μm. The relationship between the chloride concentration and the hydrostatic pressure is linear, which can be expressed as the following equation:

$$C = C_0 + bp \quad (3)$$

where C (%) is the chloride concentration in concrete, C_0 (%) is the chloride concentration without hydrostatic pressure, is the curve slope (MPa^{-1}), and is the hydrostatic pressure (MPa). Table 1 shows the values of the correlation parameters of the linear relationship.

Table 1 The values of the parameters based on Eq. (3).

Penetration depth,d (mm)	Crack width, w (μm)														
	20 μm			40 μm			60 μm			80 μm			100 μm		
	C_0	b	R^2	C_0	b	R^2	C_0	b	R^2	C_0	b	R^2	C_0	b	R^2
2.5	0.02	0.03	0.98	0.04	0.02	0.92	0.20	0.31	0.99	0.21	0.33	0.98	0.22	0.32	0.94
7.5	0.02	0.02	0.99	0.03	0.02	0.99	0.09	0.17	0.74	0.09	0.19	0.76	0.09	0.21	0.88
12.5	0.02	0.02	0.97	0.02	0.03	1.00	0.05	0.09	0.94	0.05	0.11	0.99	0.05	0.13	0.97
17.5	0.02	0.01	0.98	0.02	0.02	0.95	0.04	0.07	0.96	0.04	0.08	0.99	0.04	0.10	0.92
22.5	0.01	0.01	0.90	0.01	0.02	0.99	0.02	0.05	0.95	0.03	0.07	0.97	0.02	0.10	0.98
27.5	0.01	0.004	0.82	0.01	0.01	0.98	0.02	0.03	0.99	0.02	0.04	1.00	0.02	0.05	1.00

3.4. Diffusion coefficient

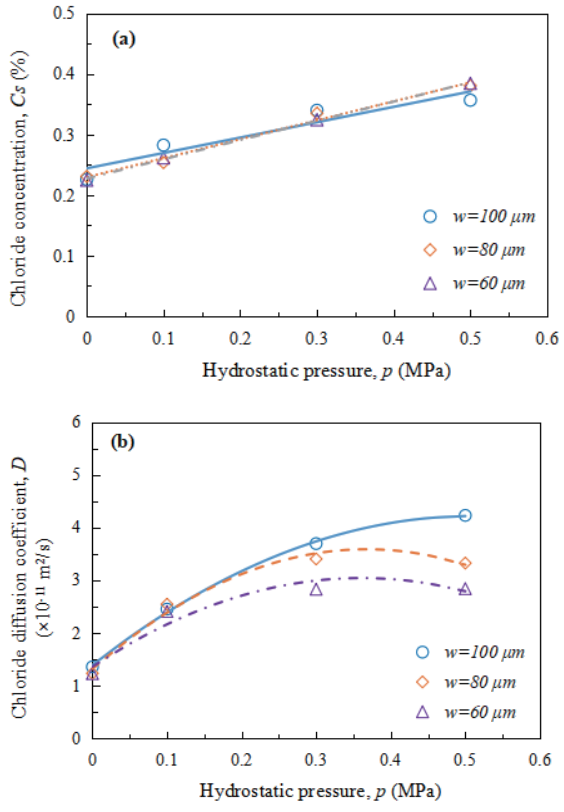


Fig. 4 Effect of hydrostatic pressure (p) on (a) chloride concentration at the concrete surface, and (b) chloride diffusion coefficent of concrete with different crack width (w).

Fig. 4a and Fig. 4b show the calculated apparent chloride diffusion coefficient and the corresponding surface chloride concentration based on Eq. (2), respectively. According to the experimental data, the chloride diffusion coefficients could not be accurately obtained since the ingress of chlorides did not follow diffusion-controlled process when the crack width was at 20 μm and 40 μm. This might be due to the fact that very little water accompanied with chlorides was able to penetrate into the small cracks and thus the ingress of chlorides does not follow a stable or unstable diffusion process. For this reason, these two sets of results are not included in Fig. 4. The chloride concentration (C_s) for the crack width from 60 μm to 100 μm increases almost linearly with increasing hydrostatic pressure. The value of at p=0 MPa is 0.22 and reaches around 0.38 at p=0.5 MPa. The effect of hydrostatic pressure on the chloride diffusion into concrete is probably due to the increase of the surface chloride concentration (C_s) in the cracks given the same chloride concentration in solution, which shows the similar trend to that illustrated in Fig. 3. Similarly, the chloride diffusion coefficient (C_a) initially increases over the increase in hydrostatic pressure, then keeps constant when the hydrostatic pressure exceeds 0.3 MPa, particularly for the crack width ranging from 60 μm to 80 μm. The results for the crack width at 20 and 40 μm are not presented here because very little change was found between these two lines and the corresponding diffusion coefficient was quite small. For the crack width of 100 μm, continuously increases as the hydrostatic pressure rises from 0 to 0.5 MPa. This suggests that the crack width promotes chloride diffusion under high hydrostatic pressure when the value exceeds 0.1 MPa. Both the calculated apparent chloride diffusion coefficient (C_a) and the

surface chloride concentration (C_s) are influenced dramatically by the hydrostatic pressure which results in the evolution of chloride diffusion as the hydrostatic pressure varies.

4. Conclusions

This study showed that hydrostatic pressure affected the chloride diffusion in the pre-cracked concrete with different crack widths. The effect of hydrostatic pressure should be considered carefully when estimating the chloride diffusion in cracked concrete and thus the chloride-induced corrosion, by which the service time of the corresponding concrete structure can be accurately predicted, and effective protective actions could be taken. The main conclusions of the study are listed below.

- Under the hydrostatic pressure from 0 MPa to 0.5 MPa, chloride concentration in the concrete increased as the crack width incremented. The chloride concentration in the concrete exhibited similar trends for the crack width ranging from 60 μm to 100 μm and for the crack width from 20 μm to 40 μm, respectively. A critical crack width seemingly exists (between 40-60 μm) beyond which the effect of hydrostatic pressure on the chloride diffusion in concrete is significantly stronger.
- For the concrete sample with a crack of width from 20 μm to 100 μm, chloride concentration increased almost linearly as the hydrostatic pressure became higher, particularly for the crack width ranging from 60 μm to 100 μm. Moreover, the increased crack width enhances the effect of hydrostatic pressure on chloride diffusion, as evidenced by the increased slope of the chloride concentration-hydrostatic pressure curve given the increase in the crack width.
- The calculated chloride diffusion coefficient and the surface chloride concentration of the cracked samples increased with increasing crack width and hydrostatic pressure.

The key engineering implications are summarized into three parts. First, a strict control of the cracks (better smaller than 40 microns) should be applied in order to minimize pressure-driven chloride attacks. Second, a pressure correction factor is suggested to be employed for chloride diffusion models for marine structures deeper than 20 meters. Third, during the concrete durability design, crack control should be prioritized by optimizing mixture proportions and adding reinforcement as well as maintaining good curing regime.

Acknowledgements:

The authors gratefully acknowledge the financial support provided by the Special projects in key areas of Guangdong Province (NO. 2023ZDZX4145), the National Natural Science Fund of China (No. 42177141), the Shandong Provincial Excellent Young Scientists Fund (2025HWYQ040), and the Research Start-up Funding Project (KYQD20250021). In addition, we would also like to express our special thanks to Shandong Provincial Key Laboratory of Oil, Gas and New Energy Storage and Transportation Safety.

References

[1] R. Wattanapornprom, T. Ishida, Comprehensive Numerical System for Predicting Airborne Chloride Generation and Its Ingress in Concrete under Actual Environmental Conditions, Journal of Advanced Concrete Technology 16(1) (2018) 18-35.

[2] H. Sun, S. Liu, F. Yu, X. Zhang, C. Wu, F. Xing, J. Ren, Behaviour of cement binder exposed to semi-immersion in chloride-rich salt solutions and seawater with different RH levels, Cement and Concrete Composites 131 (2022) 104606.

[3] K. Pasupathy, J. Sanjayan, P. Rajeev, D. Law, The effect of chloride ingress in reinforced geopolymer concrete exposed in the marine environment, Journal of Building Engineering (2021).

[4] L. Basheer, J. Kropp, D. Cleland, Assessment of the durability of concrete from its permeation properties: a review, Construction and Building Materials 15 (2001) 93-103.

[5] J. Bao, J. Wei, P. Zhang, Z. Zhuang, T. Zhao, Experimental and theoretical investigation of chloride ingress into concrete exposed to real marine environment, Cement and Concrete Composites 130 (2022) 104511.

[6] M.-Y. Chen, R.-P. Chen, Y.-Q. Chen, X. Kang, Chloride ion transport in unsaturated ultra-high performance concrete cracks under high hydraulic pressures, Construction and Building Materials 409 (2023) 133810.

[7] L. Chi, Z. Wang, Y. Zhou, S. Lu, Y. Yao, Layered Double Hydroxides Precursor as Chloride Inhibitor: Synthesis, Characterization, Assessment of Chloride Adsorption Performance, 11(12) (2018) 2537.

[8] F. Chuanqing, J. Xianyu, Y. Hailong, J. Nanguo, Theoretical and Experimental Investigation of Loading Effects on Chloride Diffusion in Saturated Concrete, Journal of Advanced Concrete Technology 13(1) (2015) 30-43.

[9] Z. He, C. He, X. Kang, X. Huang, S. Wang, Assessment of structural performance of super large cross-section subsea RC shield tunnels: Emphasis on the combined effects of highly hydrostatic pressure and corrosion-induced deterioration, Ocean Engineering 288 (2023) 116134.

[10] M.B. Otieno, M.G. Alexander, H.D. Beushausen, Corrosion in cracked and uncracked concrete - influence of crack width, concrete quality and crack re-opening, Magazine of Concrete Research 62(6) (2010) 393-404.

[11] X. Xu, D. He, S. Zeng, W. He, H. Tan, Z. Yu, Effect of concrete cracks on the corrosion of headed studs in steel and concrete composite structures, Construction and Building Materials 293 (2021) 123440.

[12] X. Wang, M. Ba, B. Yi, J. Liu, Experimental and numerical investigation on the effect of cracks on chloride diffusion and steel corrosion in concrete, Journal of Building Engineering 86 (2024) 108521.

[13] F. Du, Z. Jin, W. She, C. Xiong, G. Feng, J. Fan, Chloride ions migration and induced reinforcement corrosion in concrete with cracks: A comparative study of current acceleration and natural marine exposure, Construction and Building Materials 263 (2020) 120099.

[14] S. Wang, X. Guo, Z. Guo, C. He, X. Duan, W. Hu, K. Zhuang, Direct characterization of steel fibre corrosion in pre-cracked ultra-high performance concrete (UHPC) with different crack widths, Construction and Building Materials 315 (2022) 125769.

[15] A. Djerbi, S. Bonnet, A. Khelidj, V. Baroghel-bouny, Influence of traversing crack on chloride diffusion into concrete,

Cement and Concrete Research 38(6) (2008) 877-883.
[16] C.M. Aldea, S.P. Shah, A. Karr, Effect of Cracking on Water and Chloride Permeability of Concrete, Journal of Materials in Civil Engineering 11(3) (1999) 181-187.
[17] M. Ismail, A. Toumi, R. François, R. Gagné, Effect of crack opening on the local diffusion of chloride in cracked mortar samples, Cement and Concrete Research 38(8) (2008) 1106-1111.
[18] O.G. Rodriguez, R.D. Hooton, Influence of cracks on chloride ingress into concrete, Aci Materials Journal 100(2) (2003) 120-126.
[19] B. Gérard, J. Marchand, Influence of cracking on the diffusion properties of cement-based materials. Part I: Influence of continuous cracks on the steady-state regime, Cement & Concrete Research 30(1) (2000) 37-43.
[20] S. Jacobsen, J. Marchand, L. Boisvert, Effect of cracking and healing on chloride transport in OPC concrete, Cement and Concrete Research 26(6) (1996) 869-881.
[21] Q.-f. Liu, M.F. Iqbal, J. Yang, X.-y. Lu, P. Zhang, M. Rauf, Prediction of chloride diffusivity in concrete using artificial neural network: Modelling and performance evaluation, Construction and Building Materials 268 (2021) 121082.
[22] L.-j. Li, Q.-f. Liu, L. Tang, Z. Hu, Y. Wen, P. Zhang, Chloride penetration in freeze–thaw induced cracking concrete: A numerical study, Construction and Building Materials 302 (2021) 124291.
[23] C.-l. Zhang, W.-k. Chen, S. Mu, B. ☒avija, Q.-f. Liu, Numerical investigation of external sulfate attack and its effect on chloride binding and diffusion in concrete, Construction and Building Materials 285 (2021) 122806.
[24] Q.-f. Liu, J. Yang, J. Xia, D. Easterbrook, L.-y. Li, X.-Y. Lu, A numerical study on chloride migration in cracked concrete using multi-component ionic transport models, Computational Materials Science 99 (2015) 396-416.
[25] P.S. Mangat, K. Gurusamy, Permissible crack widths in steel fibre reinforced marine concrete, Materials and Structures 20(5) (1987) 338-347.
[26] T. Yamazaki, Y. Kajitani, Deep-sea environment and impact experiment to it, (1999).
[27] K. Li, D. Zhang, Q. Li, Z. Fan, Durability for concrete structures in marine environments of HZM project: Design, assessment and beyond, Cement and Concrete Research 115 (2019) 545-558.
[28] Ministry of Housing and Urban-Rural Development of the People's Republic of China. JGJ55-2011. Specification for mix proportion design of ordinary concrete, China Architecture & Building Press (2011-12-01).
[29] H. Zheng, M. Mooney, L. Tunstall, Pressure-driven chloride ion penetration in uncracked and cracked steel fiber reinforced concrete tunnel lining, Construction and Building Materials 470 (2025) 140616.
[30] J.M. Frederiksen, L. Mejlbro, L.-O. Nilsson, Fick's 2 nd law-Complete solutions for chloride ingress into concrete, Report TVBM-3146, Lund Institute of Technology, Sweden (2008).
[31] J.-C. Park, H.-J. Jung, Finite element method-based numerical study utilizing experimental data on chloride solution transport in concrete under hydraulic pressure, Construction and Building Materials 418 (2024) 135270.
[32] S. Chatterji, On the applicability of Fick's second law to chloride ion migration through portland cement concrete, Cement and Concrete Research 25(2) (1995) 299-303.
[33] N. Gowripalan, V. Sirivivatnanon, C.C. Lim, Chloride diffusivity of concrete cracked in flexure, Cement & Concrete Research 30(5) (2000) 725-730.
[34] L. Marsavina, K. Audenaert, G. De Schutter, N. Faur, D. Marsavina, Experimental and numerical determination of the chloride penetration in cracked concrete, Construction and Building Materials 23(1) (2009) 264-274.